Published in final edited form as:
J Vasc Interv Radiol. 2009 February ; 20(2): 241–251. doi:10.1016/j.jvir.2008.10.004.

Proteomic Profiling in Early Venous Stenosis Formation in a Porcine Model of Hemodialysis Graft

Sanjay Misra, MD, **Alex A. Fu, PhD**, **Alessandra Puggioni, MD**, **James F. Glockner, MD, PhD**, **Michael A. McKusick, MD**, **Haraldur Bjarnason, MD**, and **Debabrata Mukhopadhyay, PhD**
From the Department of Radiology and Division of Vascular and Interventional Radiology (S.M., A.A.F., A.P., J.F.G., M.A.M., H.B.) and Department of Biochemistry and Molecular Biology (D.M.), Mayo Clinic College of Medicine, 200 First Street Southwest, Rochester, MN 55905

Abstract

PURPOSE—To use proteomic analysis to identify up- and downregulated proteins in early venous stenosis formation in a porcine model of hemodialysis graft failure.

MATERIALS AND METHODS—Pigs had chronic renal insufficiency created by subtotal renal infarction caused by renal artery embolization. Arteriovenous polytetrafluoroethylene grafts were placed 28 days later and the animals were killed after a further 3 days ($n = 4$), 7 days ($n = 4$), or 14 days ($n = 4$). Proteomic analysis with isotope-coded affinity tags and multidimensional liquid chromatography followed by tandem mass spectrometry was performed on the venous stenosis and control vessels. Expression of proteins was further confirmed by Western blot analysis. The blood urea nitrogen (BUN) and creatinine levels were determined before renal artery embolization and at the time of graft placement.

RESULTS—At graft placement, mean BUN and creatinine levels were significantly higher than before embolization ($P < .05$). Six proteins were identified that were common to all four animals at the same time point. Five proteins (α-fetoprotein, fetuin A, macrophage migration inhibitory factor, pyruvate dehydrogenase E1 component, and lactoferrin) were upregulated and one protein (decorin) was downregulated. Expression of macrophage migration inhibitory factor, α-fetoprotein, and lactoferrin was further validated with Western blotting. By day 14, lactoferrin and fetuin-A expression were increased significantly in early venous stenosis formation.

CONCLUSIONS—Significantly increased expression of lactoferrin and fetuin-A were observed in early venous stenosis by day 14. Understanding the role of lactoferrin and fetuin-A in hemodialysis vascular access failure could help in improving outcomes in patients undergoing hemodialysis.

There are currently more than 400,000 patients with end-stage renal disease in the United States (1). Because of the shortage of kidneys available for renal transplantation, the vast majority of these patients require hemodialysis as the major mode of renal replacement therapy. The hemodialysis access is the “life-line” of the dialysis recipient because it is needed to allow purification of blood and maintenance of electrolyte balance. Although arteriovenous fistulas are preferred as vascular accesses for hemodialysis, expanded polytetrafluoroethylene (PTFE) arteriovenous grafts are commonly used for dialysis access in many patients. The enormity of the clinical problem lies in the lack of durability of these grafts, as only 50% of the grafts are functioning at 1 year, and only 25% at 2 years (2). Estimates suggest that hemodialysis access dysfunction has cost more than $1 billion, representing an enormous medical and financial

Address correspondence to S.M.; E-mail: E-mail: misra.sanjay@mayo.edu.
None of the authors have identified a conflict of interest.

burden on many patients (1). However, the specific mechanisms initiating venous stenosis and thrombosis remain unknown.

In patients with failed hemodialysis access, increased cellular proliferation with matrix deposition and angiogenesis has been shown to occur within the neointima and adventitia (3). These observations from clinical specimens suggest that angiogenesis plays an important role in hemodialysis vascular access graft failure. At a cellular level, many proteins have been identified to be associated with failed hemodialysis access, including vascular endothelial growth factor-A (VEGF-A), platelet-derived growth factor, transforming growth factor-β (TGF-β), basic fibroblast growth factor, and matrix metalloproteinases (MMPs) (4–9).

Identification of proteins implicated in early venous stenosis formation would be beneficial in developing therapies aimed at inhibiting venous stenosis formation. The recent development in proteomics with isotopecoded affinity tag (ICAT) labeling provides a very powerful tool to analyze all differentially expressed proteins (10,11). In the present study, we performed proteomic analysis with use of ICAT labeling in a porcine model of early venous stenosis formation in animals with chronic renal insufficiency to identify protein expression alterations (4,12,13). Next we confirmed the expression of the proteins by Western blotting. Understanding the role of these proteins in early venous stenosis formation may help improve clinical outcomes in these patients with hemodialysis access grafts.

MATERIALS AND METHODS

Study Design

Institutional animal care and use committee approval was obtained before any procedures were performed on animals. Housing and handling of the animals was performed in accordance with the Public Health Service Policy on Humane Care and Use of Laboratory Animals revised in 2000. Fourteen castrated juvenile male pigs (40–50-kg domestic swine; Larson Products, Sargeant, Minnesota) had chronic renal insufficiency created by renal artery embolization (12). Twenty-eight days later, arteriovenous PTFE grafts were placed from the carotid artery to the ipsilateral jugular vein. The proteomic changes were determined with use of cleavable ICAT labeling followed by liquid chromatography/tandem mass spectrometry at the venous stenosis and control vessels at day 3 ($n = 4$), day 7 ($n = 4$), and day 14 ($n = 4$) after graft placement. Protein expression was confirmed by Western blotting.

Creation of Chronic Renal Insufficiency by Renal Artery Embolization

Before all procedures, animals were kept without food or water for 12 hours. They were initially anesthetized with a combination of 5 mg/kg tiletamine hydrochloride (50 mg/mL) and zolazepam hydrochloride (50 mg/mL), 2 mg/kg xylazine (Bayer, Shawnee Mission, Kansas), and 0.06 mg/kg glycopyrrolate given intramuscularly. To induce additional anesthesia, an intravenous fluid line was placed in the ear vein for the delivery of zolazepam hydrochloride (5 mg/kg) as needed. During the procedure, the animals were intubated and underwent ventilation with a positive-pressure ventilator delivering oxygen (3–5 mL/kg) and isoflurane (1%–3%). The end-tidal CO_2 volume, oxygen saturation, heart rate, electrocardiographic readings, and blood pressure were monitored throughout the surgical procedure. Chronic renal insufficiency was created by subtotal renal infarction caused by embolization of the renal artery (4,12,13). The embolization procedure was standardized so the left kidney was totally embolized and the upper or lower artery was embolized. Typically, there was a single renal artery supplying each kidney with one upper- and one lower-pole branch, with each polar branch having two or three branches. The decision to embolize the right upper or lower polar artery was made based on which polar branch supplied the lesser amount of renal parenchyma. Six-French sheaths were placed in the right femoral artery and the left renal artery was selected

with use of a 5-F tapered angled glide catheter (Boston Scientific, Natick, Massachusetts). Through this catheter, 150–250-μm polyvinyl alcohol particles (Contour; Boston Scientific) and infused until the left renal artery was completely occluded. Next, the right upper- or lower-pole artery was selected and embolized completely in a similar fashion. The sheath was removed and hemostasis was obtained by manual compression. Blood urea nitrogen (BUN) and creatinine were measured before embolization, 30 minutes after embolization, and at the time of graft placement by removing 10 mL of blood from a peripheral vein. The pig was extubated, monitored postoperatively, treated for 5 days with antibiotics to prevent infection, and started on a normal pig diet (Lean Gain 95; Land O'Lakes, St. Paul, Minnesota).

Graft Placement

PTFE grafts were placed 28 days after renal artery embolization (6). Fourteen arteriovenous PTFE grafts (4 mm in diameter by 7 cm long; W.L. Gore & Associates, Flagstaff, Arizona) were placed from the right or left carotid artery to the ipsilateral jugular vein (Fig 1). The contralateral vessels were isolated surgically at the time of graft placement to serve as controls. The animals were euthanized at 3 days ($n = 4$), 7 days ($n = 4$), or 14 days ($n = 4$) after graft placement. Only patent rafts with contralateral vessels were used for proteomic analysis and Western blotting. Clopidogrel (75 mg by mouth, Bristol-Myers Squibb/Sanofi, Bridgewater, New Jersey) was started the night before the graft placement and given daily until the animal was killed.

Vessel Harvesting

To harvest the venous stenosis and control vein, the carotid and jugular vessels were dissected free of the surrounding soft tissue and a heparin bolus of 250 U/kg was given intravenously. Venous stenosis formed predictably at the vein-to-graft anastomosis. The vein-to-graft anastomosis approximately 2 cm toward the heart (venous stenosis; Fig 1) was removed as described previously (6). Circumferential tissue was removed and specimens were snapfrozen in liquid nitrogen and stored at −80°C for subsequent proteomic analysis and Western blotting.

Sample Preparation

Proteomic analysis of tissue was performed with use of cleavable ICAT labeling (Applied Biosystems, Foster City, California) followed by liquid chromatography/tandem mass spectrometry (11). Specimens from the venous stenosis and control vessels were labeled with cleavable ICAT according to the kit directions. Samples were thawed at room temperature and all graft material was removed by careful dissection and then washed three times with 1.0 mL washing buffer (0.45 mM Tris, pH 8.5). The vessels were then sliced with a surgical knife into thin pieces and then put into a denaturing buffer (0.5 mM Tris plus 0.1% sodium do-decyl sulfate). An electronic glass grinder was used to homogenize the blood vessels. The supernatant was separated by centrifugation at 14,000 rpm for 10 minutes. The protein concentration of the supernatant was measured with a protein assay kit (Bio-Rad, Hercules, California) and 100 μg of protein from each of the venous stenosis and control vessels (ie, contralateral vessels) were labeled with the cleavable ICAT. The control vein homogenates were labeled with light reagent and the venous stenosis homogenates were labeled with heavy reagent at 37°C overnight. Next, the labeled proteins from the venous stenosis and control vessels were combined and digested with equal volume of a 50 μg/mL trypsin solution at 37°C overnight. The peptide mixture then underwent further affinity purification with use of the avidin column provided with the ICAT kit. The ICAT-labeled sample was fractionated into eight fractions on an offline capillary liquid chromatography system (cap LC; Applied Biosystems) before introduction into a quadrupole time-of-flight mass spectrometer (Qstar; Applied Biosystems) for protein identification and quantification.

Protein Identification, Quantification, and Data Analysis

Protein identification was performed using the search engine from ProICAT 1.0 SP3 (Applied Biosystems) from the pig nonredundant databases. Protein quantification was obtained through Pro-ICAT software. The cutoff for the confidence settings was 75%. Each ICAT sample produced 40–50 proteins with a unique accession number. Identification of proteins was performed by selecting only those proteins common to all four animals at the same time point (ie, days 3, 7, and 14). Proteins were grouped according to the accession number. The mean stenotic: control (H:L) ratio of the common proteins present in all animals was calculated. All common proteins were manually validated for their identification and quantification based on the two precursor peaks and the charge status of the proteins. The criterion of the protein identification is based on the presence of "y" or "b" ions, at least three of each of which had to be present in the spectrum for each identified protein (14). All common proteins present in all four animals were further classified by determining the mean H:L ratio values with SD, as well as the number of peptides and their sequences (Table 1,Table 2). The upregulated proteins were defined by mean H:L ratio values greater than 1.3, and down-regulated proteins were those with mean H:L ratios less than 0.7. Each protein must have met each of these criteria to be included in the analysis, as described previously (14). However, each of these proteins was not identified in every sample and was therefore not included in the analysis. For example, MMP-2 may have been increased in three samples from day 7, but because it was not present in the fourth sample, it was not included in the final analysis.

Protein functional analysis was performed through bioinformatic procedures by "BLASTing" the National Center for Biotechnology Information Web site (http://www.ncbi.com) and searching the informatics Harvester Web site (http://www.harvester.com). Proteins with the same function were grouped according to their biologic function.

Western Blot Analysis

To confirm lactoferrin, macrophage migration inhibition factor (MIF), and α-fetoprotein protein expression, we used Western blotting on whole-vessel lysate as previously described (11). Antibodies and antisera used included lactoferrin (rabbit anti-human; Immunology Consultant Lab, Newberg, Oregon), MIF (rabbit anti-human; Abcam, Cambridge, Massachusetts), and α-fetoprotein (rabbit anti-human; Signet Lab, Dedham, Massachusetts). There is homology between the pig proteins and human proteins.

Statistical Analysis

The proteomic and Western blot data are presented as means ± SD. Analysis of variance was used first to compare the means across the day-3, day-7, and day-14 groups. If the analysis of variance F test *P* value was statistically significant ($P \leq .05$) or showed a trend toward significance, a Student *t* test was performed. The *P* values for the proteomics and Western blot groups were calculated with a one-sample Student *t* test to test the null hypothesis that the mean H:L ratio for a particular protein was different from 1. A *P* value no greater than .05 was considered to indicate statistical significance. SAS software (version 9; SAS, Cary, North Carolina) was used for statistical analyses.

RESULTS

Surgical Outcomes

Fourteen castrated juvenile male pigs weighing 48.6 kg ± 1.2 underwent total embolization of the left kidney ($N = 14$) and partial embolization of the right kidney (upper pole, $n = 2$; lower pole, $n = 12$). There were no complications as a result of the embolization procedure other than the expected induction of renal insufficiency. The BUN and creatinine levels before

embolization were 8.36 mg/dL ± 2.01 and 1.27 mg/dL ± 0.18, respectively, and at time of graft placement had increased to 17.1 mg/dL ± 9.12 and 2.17 mg/dL ± 0.57, respectively (both $P < .05$ vs before placement; Fig 2). Twenty-eight days later, 14 pigs underwent placement of 14 PTFE grafts (4 mm by 7 cm): four on the left and 10 on the right, with the contralateral vessels serving as controls.

Proteomic Analysis

Proteomic analysis with ICAT labeling was performed on venous stenotic tissue and control vessels removed from animals at day 3 ($n = 4$), day 7 ($n = 4$), and day 14 ($n = 4$). We identified six proteins common to all four animals at each time point. Of these six, five were upregulated. The upregulated group included α-fetoprotein, fetuin-A, macrophage migration inhibitory factor, lactoferrin, and pyruvate dehydrogenase E1 component (Table 1), and the downregulated group included decorin (Table 2). Table 3–Table 5 show all proteins identified at days 3, 7, and 14.

Western Blot of Lactoferrin, α-Fetoprotein, and MIF

Protein expression of lactoferrin, α-fetoprotein, and MIF was determined by Western blot in the venous stenosis and control vessels. Scanning densitometric values from the immunoblots obtained from protein samples of the stenotic vein were divided by the control vein for each time point and then normalized for protein loading (Fig 3). We observed significantly increased expression of lactoferrin (Fig 3) by day 14 ($P < .05$ for day 14 vs days 3 and 7 and for venous stenosis vs control vein). There was no statistical difference in the expression of α-fetoprotein and MIF at any of the time points.

DISCUSSION

At present, factors contributing to hemodialysis graft failure are not well understood, but are hypothesized to include changes in wall shear stress (15) and turbulent flow (16), which cause activation of matrix regulatory proteins (MMPs, VEGF-A, basic fibroblast growth factor, TGF-β, and platelet-derived growth factor), resulting in increased cellular proliferation, migration, and matrix deposition (Fig 4). Understanding early changes in protein expression in venous stenosis formation caused by hemodialysis graft failure will aid in the development of new therapies aimed at inhibiting venous stenosis formation. In the present study, we used a proteomic approach with ICAT labeling to identify and quantify differentially expressed proteins found in stenotic tissue removed from a porcine model of early venous stenosis formation. Six proteins were found that were common to all four animals at each time point. Five proteins (α-fetoprotein, fetuin-A, macrophage migration inhibitory factor, pyruvate dehydrogenase E1 component, and lactoferrin) were upregulated and one (decorin) was downregulated. From this group, the expression of four proteins was confirmed by Western blotting. We observed significantly increased levels of fetuin-A and lactoferrin by day 14 compared with other time points. Increased levels of fetuin-A have been observed in patients undergoing hemodialysis.

Fetuin-A

The serum protein fetuin-A was originally described as the major globulin in fetal and newborn calf serum (17). The human homologue was named α2–Heremans-Schmid glycoprotein after its two codiscoverers (18). Fetuin-A is a member of the cystatin superfamily of cysteine protease inhibitors. It is secreted by the liver, found in high concentrations in serum, and shown to be involved in vascular disease, atherosclerosis, hemodialysis, and inflammatory conditions (19). Fetuin-A–knockout mice have been shown to develop severe soft-tissue and intravascular calcifications (20). On a cellular level, fetuin-A is a multifunctional molecule and acts as an antagonist of TGF-β, regulating cytokine-dependent osteogenesis and inhibiting insulin

receptor tyrosine kinase and some protease activities (Fig 4) (21). It has been shown recently that it can also increase pro–MMP-9 protein secretion by monocytes, and it has been localized to arteries of patients undergoing hemodialysis (22). Increased expression of TGF-β1 has been observed in failed hemodialysis access grafts (7). In the present study, we observed significantly increased levels of fetuin A by day 14, which is in agreement with a recent study (23).

Lactoferrin

Lactoferrin is an iron-binding glycoprotein present at high levels in human milk and that of other mammals, as well as tears, saliva, bile, pancreatic juice, genital and nasal secretions, and circulating neutrophils (24). It is a multifunctional protein and is involved in protection against pathogens by having the ability to bind iron; it therefore has natural antibacterial, antifungal, and antiviral properties (25). The role of lactoferrin in vascular disease is not well understood. Increased wall shear stress occurs in veins after the placement of arteriovenous polytetrafluoroethylene grafts (15). A recent study (26) showed that, when endothelial and smooth muscle cells were cocultured together and exposed to increased shear stress, the mRNA levels of lactoferrin were increased.

Lactoferrin has been shown to inhibit angiogenesis by inhibiting basic fibroblast growth factor and VEGF-A (27). Basic fibroblast growth factor and VEGF-A have been shown to be upregulated in clinical specimens of hemodialysis graft failure (Fig 4) (8). Recent studies performed in a porcine model of hemodialysis graft failure showed increased expression of VEGF-A followed by VEGF receptor 2 and VEGF receptor 1 (13). In the present study, we observed significantly increased expression of lactoferrin by day 14 compared with days 3 and 7. However, the role of lactoferrin in hemodialysis graft failure remains unknown and needs to be investigated.

MIF

MIF is a proinflammatory cytokine that has been implicated in many inflammatory conditions including rheumatoid arthritis, cancer, and atherosclerosis (28). It is constitutively expressed by monocytes, macrophages, vascular smooth muscle cells, and endothelial cells (28). Multiple cell phenotypes are found on histologic examination of neointimal hyperplasia associated with hemodialysis graft failure (3). Although the primary cell phenotype is smooth muscle cells, occasional lymphocytes and macrophages are present (3). Macrophage migration inhibitory factor has been shown to be involved in angiogenesis mediated through the mitogen-activated protein kinase pathway and associated with increased production of angiogenic proteins such as VEGF-A and MMPs (Fig 4) (28). In addition, its cellular function includes the ability to cause increased migration of vascular smooth muscle cells and angiogenic formation through early tubule formation (28). Finally, it has been shown to be upregulated in conditions associated with oxidative stress, and increased oxidative stress is associated with hemodialysis (28).

In a murine model of atherosclerosis and angioplasty of the carotid artery, inhibiting MIF by the use of a neutralizing antibody decreased neointimal hyperplasia and cellular proliferation, which was accompanied by progressive vessel enlargement (29). In an another study performed in apolipoprotein E–deficient mice treated with neutralizing anti-MIF monoclonal antibody, there was a reduction in the local production of MMP-2 in the aorta (30). In the same model with arterial injury, it was observed that treatment with neutralizing MIF antibody resulted in a stabilization effect on the neointima with a reduction in macrophage content and an increase in smooth muscle cell content (31). In the present study, we observed increased expression of MIF in early venous stenosis formation. In a recent study (5), significantly increased expression

of MIF was observed in PTFE hemodialysis grafts, representing the end stage in the vascular stenotic process removed from patients compared with control veins.

Decorin

Decorin is a member of the family of leucine rich proteoglycans that inhibits the accumulation of extracellular matrix in models of kidney disease (32) and lung disease (33) and inhibits smooth muscle cell proliferation (34). At a cellular level, it regulates expression of many proteins, including MMPs and TGF-β1 (35). Recent studies have shown that overexpression of decorin will decrease restenosis in animal models of angioplasty-induced stenosis (36). It is also shown to be involved in angiogenesis (37). Increased expression of decorin has been found in samples removed from atherosclerotic coronary arteries (38). In the present study, we observed decreased amounts of decorin. We hypothesize that the decreased levels of decorin may be responsible for the increased cellular proliferation with increased MMP activity that has been observed in animal models of hemodialysis graft failure (Fig 4) (6). Other studies have shown *in vitro* that decorin stimulates VEGF receptor 2-and VEGF-A–mediated human umbilical vein endothelial cell proliferation and migration (Fig 4) (39). The exact role of decorin needs to be investigated in early venous stenosis formation in hemodialysis grafts.

α-Fetoprotein

α-Fetoprotein was initially described in the human fetus (40), and studies have described a role for α-fetoprotein in malignancies such as hepatocellular carcinoma (41). In gastric cancers, it has been observed that tumors that produce α-fetoprotein also secrete VEGF-A (Fig 4) (42). Increased expression of VEGF-A has been observed in clinical specimens removed from patients with failed hemodialysis vascular access (42). The role of α-fetoprotein in vascular disease has not been determined. In the present study, we observed increased levels of α-fetoprotein by proteomic analysis, which was confirmed by Western blotting. Its exact role in hemodialysis graft failure needs to be further elucidated.

Pyruvate Dehydrogenase E1

Pyruvate dehydrogenase E1 is an enzyme involved in the pyruvate dehydrogenase complex (43). It is an enzyme involved in the aerobic cellular process linking glycolysis and the citric acid cycle (43). It is stimulated by insulin and inhibited by adenosine triphosphate, nicotinamide adenine dinucleotide, and acetyl coenzyme A (43). The role of pyruvate dehydrogenase E1 in vascular disease has not been reported to date, and its role in hemodialysis graft failure needs to be determined.

There are several limitations to the present study that must be discussed. With a proteomic approach, we identified several proteins that have been implicated in hemodialysis graft failure, such as VEGF-A, MMP-2, and MMP-9 (6,9,13). However, each of these proteins was not identified in every sample and was therefore not included in the analysis. Proteomic results will provide many different proteins to be upregulated and downregulated, which can then be confirmed with Western blot analysis (10,11). We did not confirm the presence of all proteins identified by Western blot analysis.

In the present study, we used ICAT labeling with proteomic analysis to identify six proteins associated with early venous stenosis formation in a newly created model of hemodialysis graft failure. The expression of three proteins was confirmed by Western blot analysis. Finally, we observed that fetuin-A and lactoferrin were significantly increased in early venous stenosis formation. The identification of fetuin-A and lactoferrin in early venous stenosis formation provides a potential mechanism and therapeutic target for the inhibition of hemodialysis graft failure. These results provide preliminary data for further studies on determining the effect of these proteins on intimal hyperplasia in hemodialysis grafts.

Abbreviations

BUN, blood urea nitrogen; H:L stenotic:control (ratio); MIF, macrophage migration inhibition factor; MMP, matrix metalloproteinase; PTFE, polytetrafluoroethylene; TGF, transforming growth factor; VEGF, vascular endothelial growth factor.

Acknowledgments

The thank Steve Krage for help with the animal experiments and David Kallmes for the use of his laboratory.

Supported by National Institutes of Health grants CA78383, HL072178, and HL70567, and a grant from the American Cancer Society to D.M.

References

1. Collins AJ, Kasiske B, Herzog C, et al. Excerpts from the united states renal data system 2003 annual data report: atlas of end-stage renal disease in the united states. Am J Kidney Dis 2003;42(6):A5–A7. [PubMed: 14655179]
2. Schwab SJ, Harrington JT, Singh A, et al. Vascular access for hemodialysis. Kidney Int 1999;55:2078–2090. [PubMed: 10231476]
3. Rekhter M, Nicholls S, Ferguson M, Gordon D. Cell proliferation in human arteriovenous fistulas used for hemodialysis. Arterioscler Thromb 1993;13:609–617. [PubMed: 8096766]
4. Misra S, Fu A, Pugionni A, et al. Expression of hypoxia inducible factor-1a in a porcine model of chronic renal insufficiency with arteriovenous polytetrafluoroethylene grafts. J Vasc Interv Radiol 2008;19:260–265. [PubMed: 18341959]
5. Misra S, Fu A, Rajan D, et al. Increased expression of hif-1 alpha, MIF, pro MMP-2, pro MMP-9, and TIMP-1 in hemodialysis grafts. J Vasc Interv Radiol 2008;19:252–259. [PubMed: 18341958]
6. Misra S, Doherty MG, Woodrum D, et al. Adventitial remodeling with increased matrix metalloproteinase-2 activity in a porcine arteriovenous polytetrafluoroethylene grafts. Kidney Int 2005;68:2890–2900. [PubMed: 16316367]
7. Weiss MF, Scivittaro V, Anderson JM. Oxidative stress and increased expression of growth factors in lesions of failed hemodialysis access. Am J Kidney Dis 2001;37:970–980. [PubMed: 11325679]
8. Roy-Chaudhury P, Kelly BS, Miller MA, et al. Venous neointimal hyperplasia in polytetrafluoroethylene dialysis grafts. Kidney Int 2001;59:2325–2334. [PubMed: 11380837]
9. Rotmans JI, Velema E, Verhagen HJ, et al. Matrix metalloproteinase inhibition reduces intimal hyperplasia in a porcine arteriovenous-graft model. J Vasc Surg 2004;39:432–439. [PubMed: 14743149]
10. Gygi SP, Rist B, Gerber SA, Turecek F, Gelb MH, Aebersold R. Quantitative analysis of complex protein mixtures using isotope-coded affinity tags. Nat Biotechnol 1999;17:994–999. [PubMed: 10504701]
11. Misra S, Lee N, Fu A, et al. Increased expression of a disintegrin and metalloproteinase thrombospondin-1 (AD-AMTS-1) in thrombosed hemodialysis grafts. J Vasc Interv Radiol 2008;19:111–119. [PubMed: 18192475]
12. Misra S, Gordon JD, Fu AA, et al. The porcine remnant kidney model of chronic renal insufficiency. J Surg Res 2006;135:370–379. [PubMed: 16815448]
13. Misra S, Fu AA, Puggioni A, et al. Increased shear stress with up regulation of VEGF-a and its receptors and MMP-2, MMP-9, and TIMP-1 in venous stenosis of hemodialysis grafts. Am J Physiol Heart Circ Physiol 2008;294:H2219–H2230. [PubMed: 18326810]
14. Parker KC, Patterson D, Williamson B, et al. Depth of proteome issues: a yeast isotope-coded affinity tag reagent study. Mol Cell Proteomics 2004;3:625–659. [PubMed: 15047794]
15. Misra S, Woodrum D, Homburger J, et al. Assessment of wall shear stress changes in arteries and veins of arterio-venous polytetrafluoroethylene grafts using magnetic resonance imaging. Cardiovasc Intervent Radiol 2006;29:624–629. [PubMed: 16729233]

16. Abbott WM, Megerman J, Hasson JE, L'Italien G, Warnock DF. Effect of compliance mismatch on vascular graft patency. J Vasc Surg 1987;5:376–382. [PubMed: 3102762]
17. Pedersen KO. Fetuin, a new globin isolated from serum. Nature 1944;154:575.
18. Schultze HE, Heide K, Haupt H. Charakterisierung eines niedermolekularen 2-mukoids aus humanserum. Naturwiss 1962;49:15–17.
19. Ketteler M, Bongartz P, Westenfeld R, et al. Association of low fetuin-a (AHSG) concentrations in serum with cardiovascular mortality in patients on dialysis: a cross-sectional study. Lancet 2003;361:827–833. [PubMed: 12642050]
20. Schafer C, Heiss A, Schwarz A, et al. The serum protein {alpha}2-heremansschmid glycoprotein/fetuin-a is a systemically acting inhibitor of ectopic calcification. J Clin Invest 2003;112:357–366. [PubMed: 12897203]
21. Szweras M, Liu D, Partridge EA, et al. Alpha 2-hs glycoprotein/fetuin, a transforming growth factor-beta /bone morphogenetic protein antagonist, regulates postnatal bone growth and remodeling. J Biol Chem 2002;277:19991–19997. [PubMed: 11901155]
22. Tajirian T, Dennis J, Swallow C. Regulation of human monocyte proMMP-9 production by fetuin, an endogenous TGF-b antagonist. J Cell Physiol 2000;185:174–183. [PubMed: 11025439]
23. Misra S, Fu AA, Anderson J, et al. Fetuin-a expression in early venous stenosis formation in a porcine model of hemodialysis graft failure. J Vasc Interv Radiol 2008;19:1477–1482. [PubMed: 18693047]
24. Brock JH. The physiology of lactoferrin. Biochem Cell Biol 2002;80:1–6. [PubMed: 11908632]
25. Ward PP, Uribe-Luna S, Conneely OM. Lactoferrin and host defense. Biochem Cell Biol 2002;80:95–102. [PubMed: 11908649]
26. Heydarkhan-Hagvall S, Chien S, Nelander S, et al. DNA microarray study on gene expression profiles in co-cultured endothelial and smooth muscle cells in response to 4- and 24-h shear stress. Mol Cell Biochem 2006;281:1–15. [PubMed: 16328952]
27. Mader JS, Smyth D, Marshall J, Hoskin DW. Bovine lactoferricin inhibits basic fibroblast growth factor- and vascular endothelial growth factor165-induced angiogenesis by competing for heparin-like binding sites on endothelial cells. Am J Pathol 2006;169:1753–1766. [PubMed: 17071598]
28. Morand EF, Leech M, Bernhagen J. MIF: a new cytokine link between rheumatoid arthritis and atherosclerosis. 2006;5:399–411.
29. Chen Z, Sakuma M, Zago AC, et al. Evidence for a role of macrophage migration inhibitory factor in vascular disease. Arterioscler Thromb Vasc Biol 2004;24:709–714. [PubMed: 14751814]
30. Burger-Kentischer A, Gobel H, Kleemann R, et al. Reduction of the aortic inflammatory response in spontaneous atherosclerosis by blockade of macrophage migration inhibitory factor (MIF). Atherosclerosis 2006;184:28–38. [PubMed: 15921687]
31. Schober A, Bernhagen J, Thiele M, et al. Stabilization of atherosclerotic plaques by blockade of macrophage migration inhibitory factor after vascular injury in apolipoprotein e-deficient mice. Circulation 2004;109:380–385. [PubMed: 14691040]
32. Border WA, Noble NA, Yamamoto T, et al. Natural inhibitor of transforming growth factor-[beta] protects against scarring in experimental kidney disease. Nature 1992;360:361–364. [PubMed: 1280332]
33. Giri SN, Hyde DM, Braun RK, Gaarde W, Harper JR, Pierschbacher MD. Antifibrotic effect of decorin in a bleomycin hamster model of lung fibrosis. Biochem Pharmacol 1997;54:1205–1216. [PubMed: 9416971]
34. Yamaguchi Y, Ruoslahti E. Expression of human proteoglycan in chinese hamster ovary cells inhibits cell proliferation. Nature 1988;336:244–246. [PubMed: 3194009]
35. Fischer JW, Kinsella MG, Clowes MM, Lara S, Clowes AW, Wight TN. Local expression of bovine decorin by cell-mediated gene transfer reduces neointimal formation after balloon injury in rats. Circ Res 2000;86:676–683. [PubMed: 10747004]
36. Jarvelainen H, Vernon RB, Gooden MD, et al. Overexpression of decorin by rat arterial smooth muscle cells enhances contraction of type I collagen in vitro. Arterioscler Thromb Vasc Biol 2004;24:67–72. [PubMed: 14615389]
37. Nelimarkka L, Salminen H, Kuopio T, et al. Decorin is produced by capillary endothelial cells in inflammation-associated angiogenesis. Am J Pathol 2001;158:345–353. [PubMed: 11159170]

38. Riessen R, Isner JM, Blessing E, et al. Regional differences in the distribution of the proteoglycans biglycan and decorin in the extracellular matrix of atherosclerotic and restenotic human coronary arteries. Am J Pathol 1994;144:962–974. [PubMed: 8178945]

39. Kim CW, Son KN, Choi SY, Kim J. Human lactoferrin upregulates expression of kdr/flk-1 and stimulates VEGF-a-mediated endothelial cell proliferation and migration. FEBS Lett 2006;580:4332–4336. [PubMed: 16842782]

40. Bergstrand CG, Czar D. Demonstration of a new protein fraction in serum from the human fetus. Scand J Clin Lab Invest 1956;8:174. [PubMed: 13351554]

41. Motoyama T, Watanabe H, Yamamoto T, Sekiguchi M. Production of alpha-fetoprotein by human germ cell tumors in vivo and in vitro. Acta Pathol Jpn 1987;37:1263–1277. [PubMed: 2445169]

42. Kamei S, Kono K, Amemiya H, et al. Evaluation of VEGF and VEGF-c expression in gastric cancer cells producing alpha-fetoprotein. J Gastroenterol 2003;38:540–547. [PubMed: 12825129]

43. Dahl HH. Pyruvate dehydrogenase-1 alpha deficiency: males and females differ yet again. Am J Hum Genet 1995;56:553–557. [PubMed: 7887408]

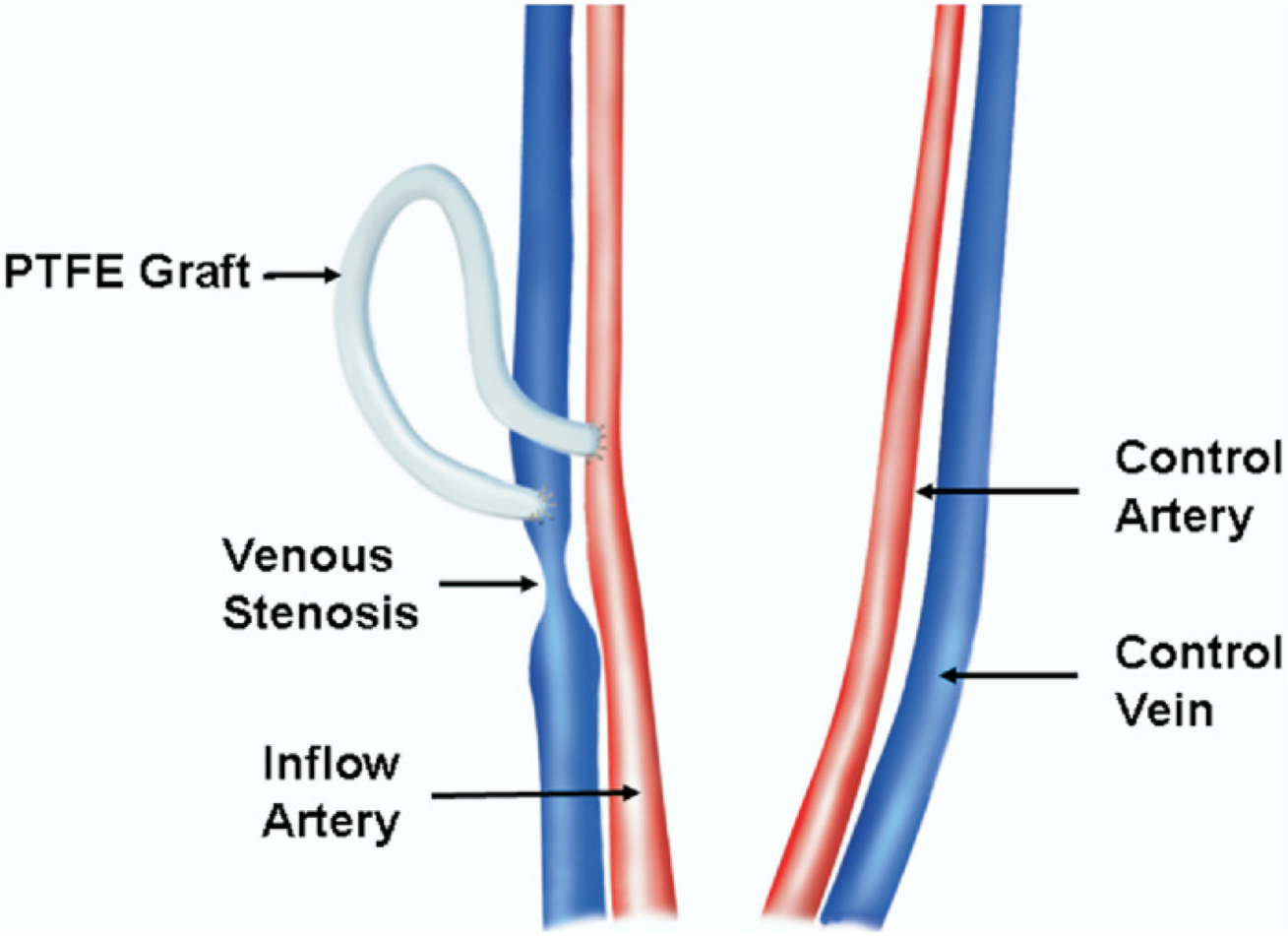

Figure 1.
Placement of PTFE hemodialysis grafts. (Available in color online at www.jvir.org.)

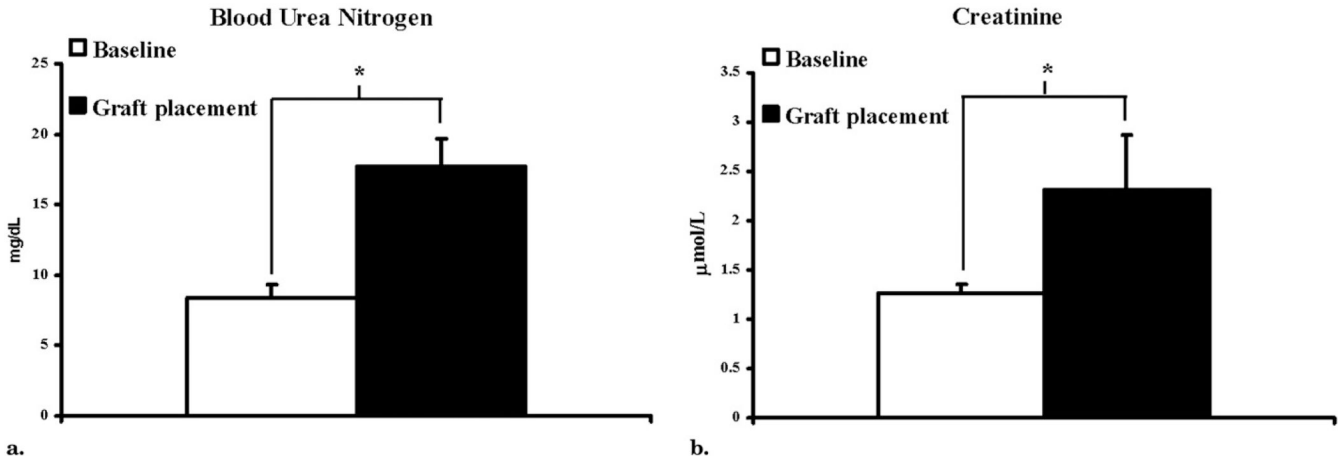

Figure 2.
Levels of BUN (**a**) and creatinine (**b**) at baseline and at placement of PTFE grafts. Data presented as means ± SD. (*$P < .05$ vs baseline.)

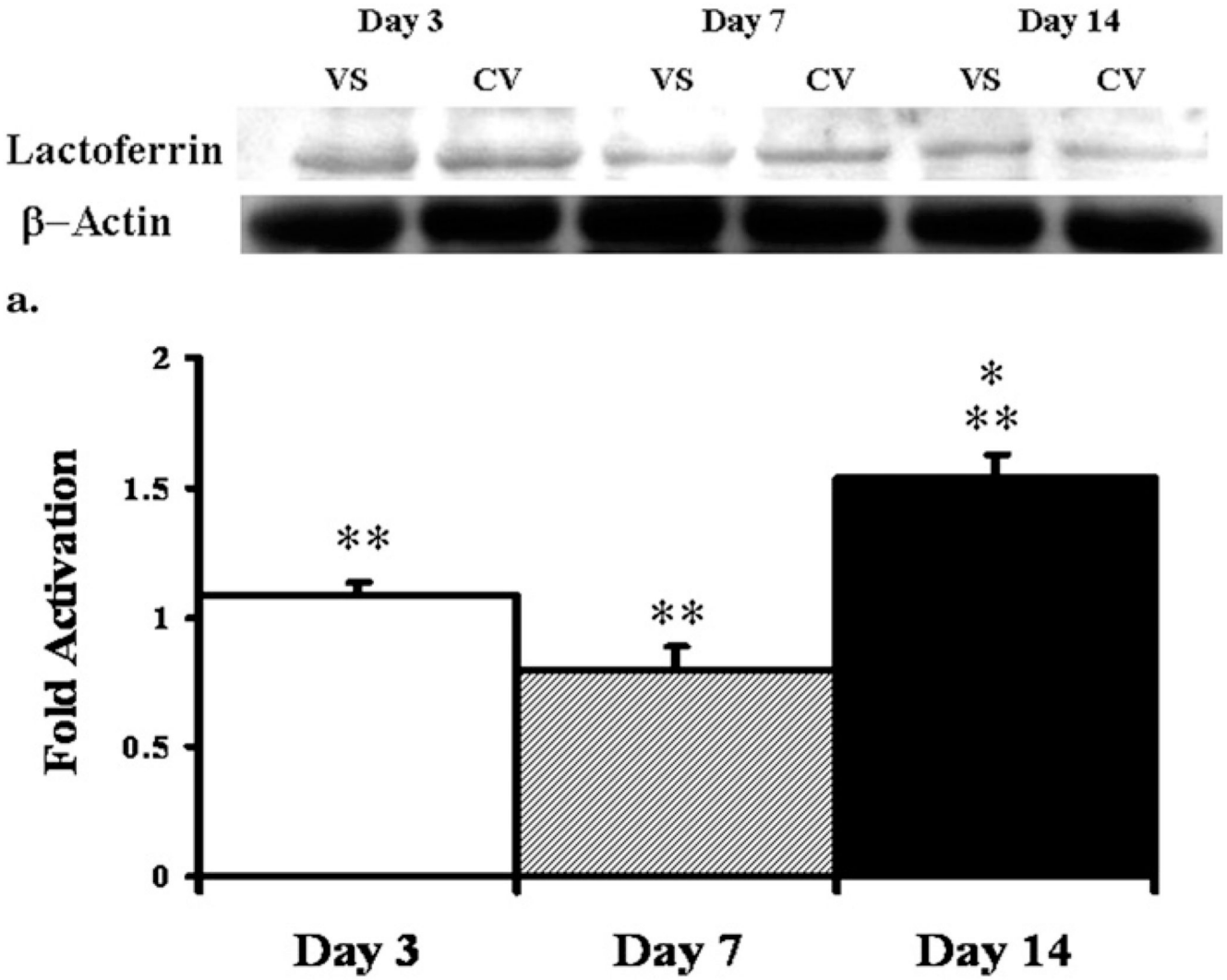

Figure 3.

Lactoferrin expression by Western blot analysis in venous stenosis and control veins. (**a**) Representative Western blot of lactoferrin at days 3, 7, and 14; lower panel shows Western blot for actin loading. *VS*, venous stenosis; *CV*, control vein. (**b**) Pooled data at days 3, 7, and 14. Data presented as means ± SD.

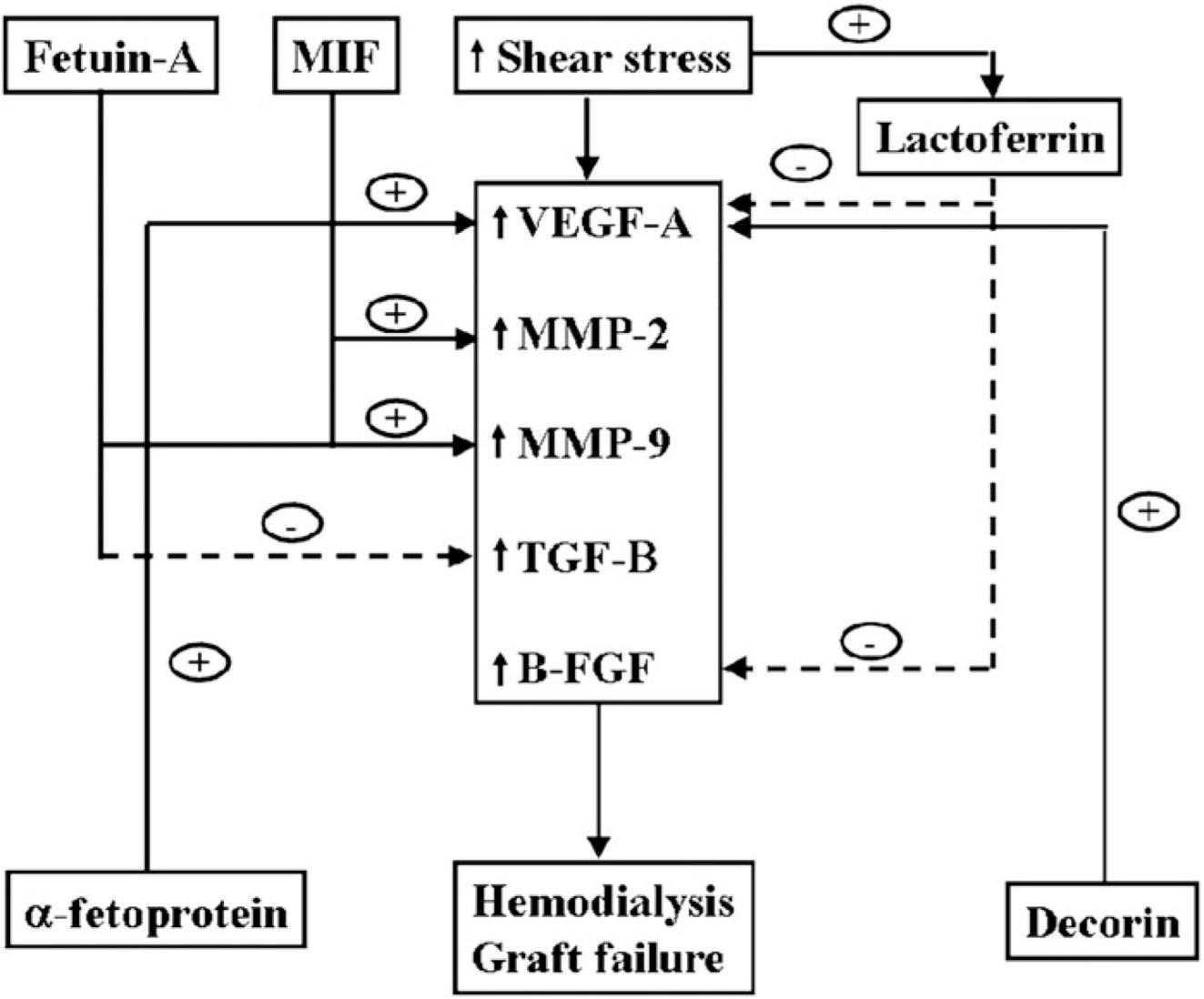

Figure 4.
Potential mechanisms of upregulated and downregulated proteins in hemodialysis graft failure.

Table 1

Upregulated Proteins in Venous Stenotic Tissue in Comparison with Controls

Accession No.	Name	Day 3	Day 7	Day 14	Peptides Found	Function
gi 191765	α-Fetoprotein	1.62 ± 1.37	1.44 ± 1.07	1.36 ± 0.27	2	Increased in hepatocellular carcinoma
gi 231467	α-2-HS-glycoprotein precursor (Fetuin-A)	1.16 ± 0.14	1.30 ± 0.63	ND	4	Protease inhibition
gi 32130529	Lactoferrin	1.31 ± 0.47	1.28 ± 0.49	1.13 ± 0.04	26	Ubiquitin protein ligase activity, zinc binding
gi 5739517	MIF	ND	1.4 ± 0.45	ND	1	Fatty acid synthesis and degradation
gi 129049	Pyruvate dehydrogenase E1 component	1.42 ± 0.24	1.19 ± 0.20	ND	1	Involved in pyruvate dehydrogenase complex

Note.—Values are presented as means ± SD where applicable. ND ± not detected.

Table 2

Downregulated Proteins in Venous Stenotic Tissue versus Controls

Accession No.	Name	Day 3	Day 7	Day 14	Peptides Found	Function
gi4929107	Decorin	ND	0.87 ± 0.74	0.60 ± 0.34	3	Inhibits smooth muscle proliferation and extracellular matrix deposition

Note.—Values are presented as means ± SD where applicable. ND = not detected.

Table 3

All Proteins Identified at Day 3

Accession No.	Name	Peptides Found	H:L Ratio
gi 15679996	Unknown (protein for IMAGE:3934797)	1	0.5814 ± 0
gi 15679996	Unknown (protein for IMAGE:3934797)	3	2.3853 ± 0.3484
gi 15679996	Unknown (protein for IMAGE:3934797)	3	0.5868 ± 0.0379
gi 15679996	Unknown (protein for IMAGE:3934797)	2	1.0067±0
gi 561819	This CDS feature is included to show the translation of the corresponding C_region. Presently transl	1	0.5493 ± 0
gi 561819	This CDS feature is included to show the translation of the corresponding C_region. Presently transl	6	2.0098 ± 0.2248
gi 561819	This CDS feature is included to show the translation of the corresponding C_region. Presently transl	6	1.2153 ± 0.0418
gi 561819	This CDS feature is included to show the translation of the corresponding C_region. Presently transl	3	1.3038 ± 0.0307
gi 33358319	CadA Orn/Lys/Arg decarboxylase, major domain	2	1.1639 ± 0
gi 33358319	CadA	3	1.2801 ± 0.0932
gi 33358319	CadA	1	1.3425 ± 0
gi 27806191	VEGF C	1	0
gi 47132317	VEGF precursor	1	—
gi 48428663	VEGF precursor (svVEGF)	1	—
gi 27464849	VEGF A	1	0.6626 ± 0
gi 11493459	PRO2619	1	0.5814 ± 0
gi 11493459	PRO2619	6	23.1722 ± 46.7707
gi 11493459	PRO2619	7	0.6245 ± 0.177
gi 11493459	PRO2619	4	1.1021 ± 0.4553
gi 2853224	Skeletal muscle LIM-protein FHL1	2	0.9697 ± 0
gi 2853224	Skeletal muscle LIM-protein FHL1	1	0.6833 ± 0
gi 2853224	Skeletal muscle LIM-protein FHL1	3	0.0504 ± 0
gi 229552	Albumin	2	0.5814 ± 0
gi 229552	Albumin	10	2.9334 ± 0.5703
gi 229552	Albumin	16	0.6206 ± 0.0509
gi 229552	Albumin	2	1.0067 ± 0
gi 45516212	COG0334: glutamate dehydrogenase	1	2.1241 ± 0
gi 45516212	COG0334: glutamate dehydrogenase	1	3.9909 ± 0
gi 45516212	COG0334: glutamate dehydrogenase	1	2.1241 ± 0
gi 45516212	COG0334: glutamate dehydrogenase	1	3.9909 ± 0
gi 125896	Ig λ-1 chain C region	1	—
gi 125947	Ig λ chain C region	2	1.4349 ± 0
gi 125947	Ig λ chain C region	3	1.2045 ± 0
gi 125947	Ig λ chain C region	1	1.2132 ± 0

Note.—Values are presented as means ± SD where applicable. Ig = immunoglobulin.

Table 4

All Proteins Identified at Day 7

Accession No.	Name	Peptides Found	H:L Ratio
gi 40062691	Pyruvate dehydrogenase	2	1.3686 ± 0.0848
gi 40062691	Pyruvate dehydrogenase	1	1.3594 ± 0
gi 40062691	Pyruvate dehydrogenase	1	1.0367 ± 0.0037
gi 40062691	Pyruvate dehydrogenase	2	1.0102 ± 0.2604
gi 45269033	Filamin	2	0.3573 ± 0
gi 45269033	Filamin	3	0.1953 ± 0.0302
gi 45269033	Filamin	3	0.5956 ± 0
gi 45269033	Filamin	4	0.4086 ± 0
gi 1236646	ch4 and secrete domains of swine IgM	2	1.3576 ± 0.0252
gi 1236646	ch4 and secrete domains of swine IgM	3	3.6031 ± 0.6975
gi 1236646	ch4 and secrete domains of swine IgM	4	1.5531 ± 0
gi 1236646	ch4 and secrete domains of swine IgM	5	1.6264 ± 0
gi 418884	Vimentin	2	1.0912 ± 0
gi 418884	Vimentin	1	1.3812 ± 0.1124
gi 418884	Vimentin	1	2.4244 ± 0
gi 418884	Vimentin	2	2.1101 ± 0
gi 26250948	Lysine decarboxylase, inducible	2	1.1626 ± 0
gi 26250948	Lysine decarboxylase, inducible	3	1.2095 ± 0.1491
gi 26250948	Lysine decarboxylase, inducible	3	0.9959 ± 0
gi 26250948	Lysine decarboxylase, inducible	4	1.002 ± 0
gi 34870650	Similar to KIAA0869 protein	1	1.0965 ± 0
gi 34870650	Similar to KIAA0869 protein	1	1.0528 ± 0
gi 34870650	Similar to KIAA0869 protein	3	1.3319 ± 0
gi 34870650	Similar to KIAA0869 protein	1	1.6719 ± 0
gi 15921674	300-aa-long conserved hypothetical protein	2	2.1376 ± 0
gi 15921674	300-aa-long conserved hypothetical protein	1	2.5881 ± 0
gi 15921674	300-aa-long conserved hypothetical protein	1	1.8388 ± 0
gi 15921674	300-aa-long conserved hypothetical protein	2	2.1585 ± 0
gi 136192	Serotransferrin (Transferrin) (Siderophilin) (β-1-metal binding globulin)	48	0.9481 ± 0.0629
gi 136192	Serotransferrin (Transferrin) (Siderophilin) (β-1-metal binding globulin)	26	1.9204 ± 0.3821
gi 136192	Serotransferrin (Transferrin) (Siderophilin) (β-1-metal binding globulin)	33	1.1997 ± 0.185
gi 136192	Serotransferrin (Transferrin) (Siderophilin) (β-1-metal binding globulin)	33	0.9055 ± 0.0954
gi 1730254	Glucocorticoid receptor (GR)	2	0.7764 ± 0
gi 1730254	Glucocorticoid receptor (GR)	1	3.9525 ± 0
gi 1730254	Glucocorticoid receptor (GR)	1	1.5809 ± 0
gi 1730254	Glucocorticoid receptor (GR)	2	0.9104 ± 0
gi 16552261	Unnamed protein product	2	1.0912 ± 0
gi 16552261	Unnamed protein product	3	2.4244 ± 0

Accession No.	Name	Peptides Found	H:L Ratio
gi 16552261	Unnamed protein product	3	2.1101 ± 0
gi 16552261	Unnamed protein product	4	1.3812 ± 0.1124
gi 32455499	RepN	2	1.203 ± 0
gi 32455499	RepN	3	1.1106 ± 0
gi 32455499	RepN	4	0.9421 ± 0
gi 32455499	RepN	5	0.9989 ± 0

Note.—Values are presented as means ± SD where applicable. aa = amino acid.

Table 5

All Proteins Identified at Day 14

Accession No.	Name	Peptides Found	H:L Ratio
gi 1203969	Filamin	5	0.2641 ± 0.0573
gi 1203969	Filamin	7	0.0737 ± 0.0208
gi 1203969	Filamin	6	0.4911 ± 0.1966
gi 1203969	Filamin	5	0.078 ± 0.0538
gi 11125367	Four and a half LIM domains 1 protein, isoform C (Zn ion binding)	3	0.2637 ± 0.0629
gi 11125367	Four and a half LIM domains 1 protein, isoform C	2	0.1595 ± 0.1021
gi 11125367	Four and a half LIM domains 1 protein, isoform C	1	0.3638 ± 0
gi 11125367	Four and a half LIM domains 1 protein, isoform C	1	0.1022 ± 0
gi 2959454	Desmin	2	0
gi 2959454	Desmin	1	—
gi 2959454	Desmin	3	0.2952 ± 0
gi 2959454	Desmin	2	0
gi 1236646	ch4 and secrete domains of swine IgM	2	2.6236 ± 0
gi 1236646	ch4 and secrete domains of swine IgM	3	1.8405 ± 0.8498
gi 1236646	ch4 and secrete domains of swine IgM	3	2.0933 ± 0
gi 1236646	ch4 and secrete domains of swine IgM	1	0
gi 1483	β-globin	4	0.6931 ± 0.0715
gi 1483	β-globin	3	0.4595 ± 0.1011
gi 1483	B-globin	5	0.5338 ± 0.0546
gi 1483	B-globin	6	0.6525 ± 0.0438
gi 15779184	FLNA protein	2	0.2824 ± 0.0623
gi 15779184	FLNA protein	2	0
gi 15779184	FLNA protein	3	0.5603 ± 0.3
gi 15779184	FLNA protein	1	—
gi 18676444	FLJ00119 protein	3	0.5603 ± 0.3
gi 18676444	FLJ00119 protein	1	—
gi 21748542	FLJ00343 protein	5	0.2641 ± 0.0573
gi 21748542	FLJ00343 protein	7	0.0737 ± 0.0208
gi 21748542	FLJ00343 protein	6	0.4911 ± 0.1966
gi 21748542	FLJ00343 protein	5	0.078 ± 0.0538
gi 23241675	ALB protein	3	1.3548 ± 0.0979
gi 23241675	ALB protein	2	1.0019 ± 0.4509
gi 23241675	ALB protein	2	5.0277 ± 0
gi 23241675	ALB protein	5	1.5889 ± 0.9452
gi 28590	Unnamed protein product	3	1.3548 ± 0.0979
gi 28590	Unnamed protein product	2	1.0019 ± 0.4509
gi 28590	Unnamed protein product	2	5.0277 ± 0
gi 28590	Unnamed protein product	5	1.5889 ± 0.9452

Accession No.	Name	Peptides Found	H:L Ratio
gi 33592823	Conserved hypothetical protein	3	1.2998 ± 0
gi 33592823	Conserved hypothetical protein	1	1.2071 ± 0
gi 33592823	Conserved hypothetical protein	4	1.4004 ± 0.064
gi 33592823	Conserved hypothetical protein	3	1.5191 ± 0.197
gi 38087063	Similar to filamin	3	0.2824 ± 0.0623
gi 38087063	Similar to filamin	2	0.0632 ± 0
gi 38087063	Similar to filamin	3	0.5603 ± 0.3
gi 38087063	Similar to filamin	2	0
gi 1255995	Heat shock cognate 70.I	1	—
gi 1255995	Heat shock cognate 70.I	1	5.0544 ± 0
gi 7637387	Heat shock protein	1	1.7406 ± 0
gi 7637387	Heat shock protein	1	—
gi 178345	Alloalbumin Venezia	3	1.3548 ± 0.0979
gi 178345	Alloalbumin Venezia	2	1.0019 ± 0.4509
gi 178345	Alloalbumin Venezia	2	5.0277 ± 0
gi 178345	Alloalbumin Venezia	5	1.5889 ± 0.9452

Note.—Values are presented as means ± SD where applicable. Ig = immunoglobulin.